Published in final edited form as:
J Neurol Sci. 2009 October 15; 285(1-2): 28–38. doi:10.1016/j.jns.2009.04.041.

Myofibrillar protein and gene expression in acute quadriplegic myopathy

Holly Norman[a], **Håkan Zackrisson**[b], **Yvette Hedström**[a], **Per Andersson**[a], **Jenny Nordquist**[a], **Lars I. Eriksson**[c], **Rolf Libelius**[d], and **Lars Larsson**[a,e,*]

[a]Department of Clinical Neurophysiology, Uppsala University, Sweden

[b]Karolinska Institute, Stockholm, Sweden

[c]Department of Anesthesiology, Karolinska Institute, Stockholm, Sweden

[d]Department of Clinical Neurophysiology, Umeå University, Sweden

[e]Center for Developmental and Health Genetics, Pennsylvania State University, University Park, PA, USA

Abstract

The dramatic muscle wasting, preferential loss of myosin and impaired muscle function in intensive care unit (ICU) patients with acute quadriplegic myopathy (AQM) have traditionally been suggested to be the result of proteolysis via specific proteolytic pathways. In this study we aim to investigate the mechanisms underlying the preferential loss of thick vs. thin filament proteins and the reassembly of the sarcomere during the recovery process in muscle samples from ICU patients with AQM. Quantitative and qualitative analyses of myofibrillar protein and mRNA expression were analyzed using SDS-PAGE, confocal microscopy, histochemistry and real-time PCR. The present results demonstrate that the transcriptional regulation of myofibrillar protein synthesis plays an important role in the loss of contractile proteins, as well as the recovery of protein levels during clinical improvement, myosin in particular, presumably in concert with proteolytic pathways, but the mechanisms are specific to the different thick and thin filament proteins studied.

Keywords

Myosin; Actin; Myosin binding proteins; Acute quadriplegic myopathy; mRNA

1. Introduction

Acute quadriplegic myopathy [1] is a disease associated with prolonged mechanical ventilation, unloading of limb muscles and the administration of corticosteroids (CS) or neuromuscular blocking agents [2,3] or both in combination [4–6] with an underlying systemic illness. Typically, AQM is recognized when intensive care unit (ICU) patients are slow to wean from the mechanical ventilator [3]. Clinical characteristics include flaccid muscle paralysis of limb muscles, muscle wasting, intact cranial nerve function, low compound muscle action potentials and intact motor and sensory nerve conduction velocities

*Corresponding author. Department of Clinical Neurophysiolgy, Uppsala University Hospital, Entrance 85, 3rd Floor, 751 85 Uppsala, Sweden. Tel.: +46 18 611 3445; fax: +46 18 556 106. lars.larsson@neurofys.uu.se (L. Larsson).

[5,7,8]. Other pathological features include a preferential loss of the thick filament protein myosin [4,5,7,9–11], muscle fiber atrophy [3–5], and an in-excitable muscle membrane [8].

AQM is associated with increased mortality [6,12], slow recovery over a period of weeks to several months [3,4], severely impaired quality of life and increased health care costs [13]. After recovery from the primary disease and elimination of the causative factors, patients typically recover from muscle paralysis, but recovery may take several months and it is not uncommon that patients never regain their pre-ICU muscle function [14–16], thus impairing their functional ability permanently. In fact, functional limitations were shown to persist in the majority of patients as late as 2 years post-AQM, which was largely a result of muscle wasting and weakness [17,18].

The rapid muscle wasting in patients with AQM has been suggested to be associated with the activation of the ubiquitin–proteasome, cytoplasmic (calpain), and lysosomal (cathepsin) proteolytic pathways [11,19–24]. The muscle atrophy in AQM also is distinguished from neurogenic atrophy by the activation of the MAPK signaling cascade, including the proapoptotic transforming growth factor (TGF)-β and RAS cascades, as demonstrated by Di Giovanni and co-workers [19].

In contrast to the generally accepted role of protein degradation and muscle wasting in AQM [22,24–26], the importance of protein synthesis regulation has received little attention. In patients with AQM, a dramatic down-regulation of all adult skeletal myosin heavy chain (MyHC) isoforms at the mRNA level and an intact transcription of the dominating thin filament protein actin was observed in the acute phase with generalized muscle paralysis, and restoration of MyHC transcript levels during recovery of muscle function according to *in situ* hybridization [7]. A more complete understanding of the mechanisms underlying the preferential loss of myofibrillar proteins, in particular the thick filament protein myosin, and the consequent loss of functional capacity of skeletal muscle is of significant interest in the design of intervention and prevention strategies.

The aim of this study was to improve our understanding of the transcriptional regulation of myofibrillar protein synthesis in spinal nerve innervated limb muscles in ICU patients with AQM and during the recovery process. We hypothesized that the down-regulation of protein synthesis at the transcriptional level plays an important role for the preferential loss of thick filament proteins in limb muscles from patients with AQM. Specific interest is focused on myosin protein and mRNA expression at the biopsy and single muscle fiber levels. Analyses have been extended to also include the myosin associated thick filament proteins, myosin binding proteins C and H (MyBP-C, MyBP-H), and the dominating thin filament protein actin. Additionally, a rare case of the effects of AQM and recovery, compared to a previously taken biopsy in the same individual are presented. The results from this study have been published in abstract form elsewhere [27].

2. Materials and methods

2.1. Patients and control subjects

A total of seven patients, four females and three males, aged 58–75 years, were included in this study (Table 1). All patients were characterized by severe generalized muscle weakness or complete paralysis of all limb and trunk muscles and normal or only slightly impaired function of cranial nerve innervated muscles. Diagnosis was based on electrophysiology, histopathological analyses of muscle biopsies, clinical history and observations. The patients are numbered M1–M7 and four of these patients have been included in a previous study [28]. This study was approved by the local Ethical Committees on Human Research at the

Karolinska Hospital, Stockholm, and Uppsala University Hospital, Uppsala, Sweden and the ethical committee of the Pennsylvania State University, University Park, PA, USA.

A total of 22 healthy control subjects, 13 females and 9 males, were included for comparison. Age ranged between 24–80 years. All biopsies, excluding 2 of which had an acute peripheral neuropathy, were free of locomotor and neuromuscular disease. Samples from the tibialis anterior muscle were analyzed from eight of the control subjects and from the vastus laterlis muscle in the remaining 14 subjects. Samples were age, sex and muscle type matched.

2.2. Muscle biopsy

Biopsy samples were obtained from the tibialis anterior or vastus lateralis muscle using the percutaneous conchotome method. Each biopsy was dissected free of fat and connective tissues and divided into two portions. One portion was frozen in either Freon or isopentane cooled by liquid nitrogen and stored at −80 °C for later analyses. Small bundles of 25–50 fibers were dissected from the other portion of the biopsy material and treated as previously described [29]. Muscle bundles were snap frozen with either Freon or isopentane cooled by liquid nitrogen and stored at −80 °C.

2.3. Enzyme-histochemistry and immunocytochemical techniques

The frozen muscle samples were cut at the greatest girth perpendicular to the longitudinal axis of the muscle fibers into 10 μm thick cross-sections with a cryotome (2800 Frigocut E, Reichert-Jung GmbH, Heidelberg, Germany) at −20 °C. The sections were stained with the following histochemical and immunnocytochemical reactions: myofibrillar ATPase (mATPase) after acid (pH 4.6) pre-incubations [30,31], acid phosphatase [32], monoclonal antibodies (mAbs) against embryonic (G6), fetal (B6), slow- (A4.951) and fast-myosin (A4.74) heavy chain isoforms [33,34] and mAbs against Leu-19 and ubiquitin (U 6253) Sigma. The primary antibody was identified by anti-mouse Ig conjugated by peroxidase-anti-peroxidase (PAP) coupled to a biotin–avidin complex. Cross-sectional areas (CSA) and lesser fiber diameter (d_{min}) of individual muscle fibers [32] were measured using a semiautomatic technique applied to black-and-white photographs of mATPase stained muscle cross sections (Kontron, Bildanalyse GmbH, Munich FRG). When possible 100 type I fibers and 50 fibers of each of the type II subtypes were measured from each biopsy.

Both enzyme-histochemical and immunocytochemical techniques were used to study the spatial distribution of regions unreactive with mATPase or mAbs, i.e., the same fibers were identified on 200, 10 μm cross-sections of a single muscle biopsy. The mATPase staining was restricted to one acid preincubation (pH 4.6) to ensure that sections were in close vicinity along the longitudinal axis of the muscle fibers to facilitate accurate comparison between enzyme-histochemical and immunocytochemical stainings.

2.4. Gel electrophoresis

Gel electrophoresis was performed to measure the protein contents in both muscle cross-sections and single fibers. 12% sodium dodecyl sulfate-polyacrylamide gel electrophoresis (SDS-PAGE) [35] was run for the measurement of both myosin and actin protein content, as well as for western blots (discussed below), while 6% SDS-PAGE was run to determine myosin heavy chain isoform protein expression. The gel matrix has been described previously [35]. Briefly, electrophoresis was performed at a constant current of 16 mA for 5 h with a Tris–glycine electrode buffer (pH 8.3) at 15 °C (SE 600 vertical slab gel unit, Hoefer Scientific Instruments, San Francisco, USA).

For measuring the protein contents of muscle biopsies, two 10 μm cross-sections of each sample were dissolved in urea buffer (8 M; 120 g Urea, 38 g thiourea, 70 ml H_2O, 25 g mixed bed resin, 2.89 dithiothreitol, 1.51 g Trizma base, 7.5 g SDS) and run on a 12% SDS-PAGE [35]. To measure the myosin and actin protein contents in single fibers, individual fibers were dissolved in urea buffer (8 M), a portion of which was subsequently loaded onto a 12% SDS-PAGE and the remainder subjected to total protein quantification (see below). A standard curve with 5 dilutions (range 12.5 ng–200 ng) of purified myosin (My02, Cytoskeleton, Inc., MediQip, Huddinge, Sweden) and actin (AKL99, Cytoskeleton, Inc., MediQip, Huddinge, Sweden) was included on each gel to quantify the amount of protein.

Gels, i.e., 12%, were stained with Coomassie blue [36], which was chosen due to high reproducibility and the ability to penetrate the gel and stain all proteins present, i.e., allowing accurate quantitative protein analyses [36]. Alternatively, separating gels for 6% SDS-PAGE were silver-stained, due to high sensitivity [37]. All gels were subsequently scanned in a soft laser densitometer (Molecular Dynamics, Sunnyvale, CA, USA) with a high spatial resolution (50 μm pixel spacing) and 4096 optical density levels. The volume integration function was used to quantify the amount of protein on 12% and 6% gels (ImageQuant TL Software v. 2003.01, Amersham Biosciences, Uppsala, Sweden). These values were used to calculate myosin:actin protein ratios in both whole biopsies and single fibers, as well as to relate the amount of myosin and actin to the total protein of each fiber (see below), and to quantify the percentage of each myosin isoform in whole biopsies.

Each myosin isoform band on a 6% SDS-PAGE was quantified using a laser densitometer. The amount of each isoform, in relation to the total MyHC, was determined and calculated to be a percentage of total MyHC, thus determining the myosin isoform composition. The mRNA expression value (isoform specific) was then equivocated to the corresponding percentage protein expression of the specific isoform and used to calculate the total MyHC mRNA for MyHC:actin mRNA ratios, since the skeletal MyHC mRNA expression parallels, in relative intensity, the MyHC protein expression [38–40].

2.5. Protein quantifications

To quantify the total protein of single muscle fibers, fibers were dissected after de-sucrose treatment [29] and submerged into 10 μl urea buffer (8 M), with subsequent centrifugation and heating (90 °C for 2 min). This sample was then used for total protein quantification using the NanoOrange® Protein Quantification Kit (Molecular Probes, Inc., Eugene, OR, USA). The fluorescence of the samples was measured using a Plate Chameleon™ Multilabel Platereader (Hidex Oy, Finland) and related to a standard curve. Values were calculated using the software MikroWin, version 4.33 (Microtek Laborsysteme GmbH, Overath, Germany).

Single fiber myosin and actin quantities were calculated from a 12% gel, which included a 5 point standard curve (see above), and then divided by the total protein content in the fiber. Approximately 10 fibers were run from each biopsy and the values from these fibers were averaged to gain the single fiber myosin and actin content, as well as the myosin:actin ratio, for each patient (Table 2).

Gel electrophoresis (12% SDS-PAGE; Coomassie stained) was performed on muscle biopsy cross sections to quantify MyBP-C. The MyBP-C protein expression was normalized to total protein content using a soft laser densitometer (Molecular Dynamics, Sunnyvale, California, USA).

2.6. Quantitative real-time PCR

The RNA for quantitative real-time PCR was extracted from frozen muscle tissue (5–10 mg) using Qiagen RNeasy® Micro Kit (Qiagen, Inc., Valencia, CA, USA). Muscle tissue was homogenized using a rotor homogenizer (Eurostar Digital, IKA-Werke). QIAshredder™ columns (Qiagen Inc., Valencia, CA, USA) were used to disrupt DNA. Total RNA was eluted from RNeasy® Mini columns with 12 μl of RNase-free water. RNA-concentrations were then quantified using the fluorescent nucleic acid stain, Ribogreen® (Molecular Probes, Eugene, OR, USA), on a Hitachi F-4000 fluorescence spectrophotometer.

cDNA was prepared using Ready-To-Go™ You-Prime First-Strand-Beads (Amersham Biosciences, Uppsala, Sweden) according to the instructions from the manufacturer. Total RNA (100 ng) was used to synthesize cDNA, using 0.66 μg random hexamers (Amersham Biosciences, Uppsala, Sweden) and 0.5 μg oligo-dT primers (Amersham Biosciences, Uppsala, Sweden). The cDNA was diluted to a volume of 100 μl and stored at −80 °C until quantification by RT-PCR.

Real-time PCR was used to quantify the mRNA levels for human embryonic, fetal (perinatal), type I, IIa, and IIx MyHCs, skeletal α-actin, myosin binding protein C (MyBP-C; both fast and slow isoforms) and myosin binding protein H (MyBP-H; GenBank accession AF111784, AF111785, M58018, NM_002472, NM_00247, NM_001100, NM_004533, NM_002465, NM_004997, respectively). Taqman primers and probes were designed using the software Primer Express® (Applied Biosystems, Foster City, CA, USA). Sequences for primers and probes are listed in Table 3. Probes, labelled with FAM (*N*-(3-fluoranthyl)maleimide), and primers were purchased from Thermo Electron (Thermo Electron GmBH, Ulm, Germany). All primers and probes were HPLC purified. SYBR Green (1988123, Roche Diagnostics GmbH, Germany) was used for detection of MyBP-H, MyBP-C_{fast} and MyBP-C_{slow} as well as for 28 S when used as a standard for MyBP-H and MyBP-C (fast and slow isoforms).

Real-time PCR was run using a MyiQ™ PCR detection system (Bio-Rad Laboratories, Inc., Hercules, CA, USA) with AmpliTaq® Gold DNA polymerase (Applied Biosystems, Foster City, CA, USA). When optimizing each PCR, PCR products were run on 2% agarose gels to ensure that primer-dimer formation was not occurring. Only one product of expected size was detected in all cases. Each sample was run in triplicates. With each PCR run, a standard cDNA was included in triplicates of three concentrations comprising a standard curve. A control sample was used for the standard. Finally, negative controls without cDNA were included on each plate.

Sequence detection software 1.0.410 (Bio-Rad Laboratories, Inc., Hercules, CA, USA) was used to analyze the raw real-time PCR data. The threshold cycle (C_T) data acquired for each sample was related to the standard curve to obtain the starting quantity (SQ) of the template cDNA for each sample. Each sample in a triplicate had to be within 0.5 C_T of each other to be included in the analysis. The SQ of the sample was divided by the standard SQ, 28 S (GenBank accession M11167). Sequences for 28 S primers and probe are listed in Table 3. Standard curves for both the gene of interest and 28S were included on each plate. To be accepted, slopes of the standard curves had to be between −3.0 and −3.5 and were not allowed to differ by more than 5%. The values of the samples, related to the standard, were then analyzed.

2.7. Statistics

Mean and standard deviations (SD) were calculated by standard procedures. A t-test was performed to compare the acute stage patients and controls; however, when the normality test failed a Mann Whitney Rank Sum test was performed. One way analysis of variance

(ANOVA) was used to compare all groups to controls. When the normality test failed, a one way ANOVA on ranks, i.e., Kruskal–Wallis one way ANOVA, was used. ATukey's *post-hoc* contrast was performed to determine the means that were different at the significance level of $p<0.05$; when normality failed, Dunn's *post-hoc* was used. Values were excluded if they varied more than 2 standard deviations from the mean. Differences were considered significant at $p<0.05$.

3. Results

3.1. Patients

In the acute phase of AQM, the following features were shared by the patients: 1) generalized muscle weakness or complete paralysis of all limb and trunk muscles, while craniofacial muscle function was not, or significantly less, affected, 2) intact sensory and cognitive function (when this could be tested), 3) exposure to mechanical ventilation, prolonged high-dose systemic CS treatment, 4) NMBA treatment, albeit in highly variable doses ranging from one single dose to prolonged administration for more than two weeks, 5) improvement in muscle function after the initial period with complete or near complete muscle paralysis, and 6) low or absent compound muscle action potentials upon supramaximal stimulation of the motor nerve at the time of the first examination when the patients showed generalized muscle weakness/paralysis.

3.2. Histopathology

One or more of the following histopathological findings were observed in all patients: atrophic, angular, necrotized muscle fibers with fat infiltration, vacuolization, unstained sarcoplasmic areas with no mATPase reactivity and fibers with no or only diffuse reactivity with mATPase staining. In some patients, almost all muscle fibers were unreactive in the mATPase staining, at the time of the first biopsy. In others, specific areas revealed variable mATPase staining intensity, ranging from a weaker than normal to complete loss of mATPase stainability with surrounding fibers displaying normal staining pattern (Fig. 1). These findings were confirmed by immunocytochemical stainings using mAbs reactive with fast or slow myosin epitopes. The unstained regions of the muscle fibers were not restricted to a specific muscle fiber type, i.e., unstained regions were observed in muscle fibers expressing fast, slow, embryonic or fetal myosin isoforms.

In the acute phase all patients demonstrated signs of mild lysosomal proteolysis according to acid phosphatase staining and a variable reactivity with leu-19 (a marker for satellite cell activation and repair), embryonic (G6) and fetal (B6) myosin antibodies, markers for muscle fiber regeneration. A variable reactivity pattern in these different markers of muscle regeneration was observed between the different patients. The relative number of Leu-19, G6 and B6 reactive fibers varied between 10–20%, 10–50% and <5–20% respectively. All B6 and Leu-19 reactive fibers were reactive with G6 mAbs, but there were several G6 reactive fibers unreactive with B6 and Leu-19.

At the time of the first biopsy, the average muscle fiber size was reduced in all patients, but the atrophy was highly variable between patients and ranged from severe to mild. Despite the complete or near complete loss of mATPase staining or MyHC immunoreactivity, intrafusal muscle spindle fibers appeared to be spared from the myosin loss according to mATPase and immunocytochemical stainings (Fig. 2). During early recovery at the time of the second biopsy 1–2 months after admission to ICU, patients had weaned from the respirator. They could activate some limb muscles voluntarily, but were still too weak to stand or walk. All muscle biopsies revealed muscle fibers with mATPase staining and myosin monoclonal antibody reactivity, but pathological findings were also observed in all

patients, including central nuclei, atrophic fibers with unstained regions, irregular form and vacuolization (Fig. 3). Signs of muscle fiber regeneration were only observed in three of the patients during early recovery and the relative number of Leu-19, G6 and B6 reactive fibers varied between 5–40%, 10–70% and 5–50%, respectively. According to acid phosphatase staining, lysosomal proteolysis was still activated in early recovery. According to immunocytochemical stainings, the ubiquitin proteolytic pathway was activated in only one patient (M1) during early recovery. Muscle biopsies were taken from three of the patients after complete recovery, 4–12 months after admission to the ICU. At this time there were no signs of myopathy and fibers showed normal mATPase activity and myosin monoclonal antibody reactivity.

3.3. Myofibrillar protein analyses

At the muscle biopsy level, the myosin:actin ratio was significantly decreased ($p<0.01$) during the acute stage compared with age-matched healthy controls, qualitative findings at the single cell level also included disorganized sarcomere and myonuclei pattern and a decreased myosin staining intensity (Fig. 1). After 1–2 months recovery, the myosin:actin ratio had returned to the control value and only fluctuated slightly during the latter recovery points, most likely due to small sample size (Fig. 1). In agreement with this finding, the patient with a pre-AQM biopsy had a normal myosin:actin ratio at the first post-AQM recovery time point of 5 months (Fig. 4).

The total decrease of MyHC during AQM was not characterized by any significant preferential change in the expression of an individual isoform expressed in human skeletal muscle, i.e., type I, IIa and IIx MyHCs, with all isoforms decreasing dramatically. Further, MyBP-C, the most abundant protein in the thick filament, next to myosin, was also lost or decreased in the acute phase of AQM (Fig. 5). In spite of the decreased MyBP-C expression, MyBP-H was not found to be decreased during the acute phase and subsequent recovery phases according to qualitative Western blot analyses (data not shown).

At the single muscle fiber level, the concentration of myosin protein was decreased ($p<0.001$) in all patients during the acute stage compared with controls. In those patients where myosin concentrations were measured at the single muscle fiber level, myosin expression increased gradually during the recovery process but did not reach normal levels until late stage of recovery, i.e. after 8–12 months. Actin content, on the other hand, was only decreased ($p<0.001$) in 4 out of the 7 patients in the acute stage of AQM, although the overall average actin content was decreased ($p<0.001$; Table 2). Further, actin contents returned to normal at a faster rate than myosin during the recovery process (Table 2). Contrasting to the results of myosin:actin ratios at the muscle biopsy level, the myosin: actin ratio remained decreased until the 8–12 month time point at the single fiber level (Table 2).

3.4. Myofibrillar protein mRNA expression

MyHC I and IIa mRNA expression, the dominating MyHC isoforms of the tibialis anterior, decreased ($p<0.05$) during the acute stage, compared to age-matched healthy controls. After 1–2 months recovery, there was a marked increase in MyHCI and IIa mRNA expression. After 4–5 months recovery, MyHC mRNA levels appeared to peak and returned to normal levels after 8–12 months (Figs. 6 and 7).

Fetal MyHC mRNA expression did not differ significantly between acute and control biopsies; however, at 1–2 months recovery fetal MyHC increased significantly ($p<0.05$) and returned to control values by 8–12 months (Fig. 6). Embryonic MyHC mRNA was not detectable in controls or in patients during the acute phase of AQM. During early recovery, embryonic MyHC mRNAwas visible, but values were too low to allow reliable

quantification. This is consistent with the temporal sequence of embryonic and fetal MyHC isoform expression reported during myogenesis [41] as well as the expression of embryonic MyHC according to immunocytochemistry, i.e., the faster down-regulation of embryonic vs. fetal mRNA expression and the slow turnover rate at the protein level.

Total MyHC mRNA content was lower ($p<0.01$) in the acute phase of AQM compared with controls. During recovery, total MyHC mRNA tended to increase prior to returning to values similar to controls at late stages of recovery (Fig. 7A).

Actin mRNA decreased significantly ($p<0.05$) during the acute stage compared to control values and returned to normal values during recovery (Fig. 7B).

There was no statistically significant difference in MyBP-C_{fast} and MyBP-C_{slow} mRNA expression between patients and controls (Fig. 8). On the other hand, there was a slight trend ($p=0.08$) towards an up-regulation of MyBP-H mRNA expression during early recovery compared with age-matched healthy controls (Fig. 8). This is consistent with MyBP-H protein expression on Western blots, as well as recent data demonstrating increased MyBP-H mRNA levels in a rodent AQM model [42].

4. Discussion

Severe muscle wasting and impaired muscle function accompany critical illness in ICU patients with negative consequences for recovery from primary disease and weaning from the respirator. While ICU outcome has traditionally focused simply on survival, modern critical care also addresses post-ICU complications and quality of life. Several recent studies show unambiguously that neuromuscular dysfunction, resulting in muscle wasting and weakness, is the most persistent and debilitating of problems for survivors from the ICU for as long as two years after hospital discharge, which is the longest observation period reported to date [17,18]. There is, therefore, a significant need for more research focused on the mechanisms underlying the muscle wasting and weakness in ICU patients [43]. The dramatic muscle wasting, preferential loss of myofibrillar proteins and impaired muscle function in ICU patients with AQM have traditionally been suggested to be the result of proteolysis via specific proteolytic pathways [19,44,45]. The present results demonstrate that the transcriptional regulation of myofibrillar protein synthesis plays an important role in the loss of contractile proteins, as well as the recovery of protein levels during clinical improvement, myosin in particular, presumably in concert with proteolytic pathways.

4.1. Myosin loss in ICU patients

ICU patients with an acquired myopathy and generalized muscle weakness have been divided into three groups based on biopsy findings: i) myopathic appearance with increased fiber size variability, internal nuclei, maintained differentiation of muscle fiber types according to myofibrillar ATPase (mATPase) staining, ii) focal or general loss of myofibrillar ATPase staining and electronmicroscopy reveal focal or general loss of thick filament proteins such as myosin, and iii) necrotizing myopathy with leakage of CK and myoglobin resulting in elevated serum levels for longer than a week [44,45]. It is not known if these three types of myopathies represent clinical manifestations with a common pathophysiology, but various severities, or if they represent different entities [44]. The different patients included in this study can be divided into these three categories based on results from histopathological analyses of muscle biopsy sections, S-CK and myoglobin values.

Electrophoretic separation of myofibrillar proteins demonstrated a preferential loss of myosin in all patients, despite the fact that only minimal changes were observed in the

mATPase staining pattern in some patients. The preferential loss of myosin in all of the three groups lends support to the concept that the three different myopathies described above represent different levels of severity of the same disease. Further, the only patient in this study with signs of rhabdomyolysis also had the poorest recovery of muscle function during the recovery process and remained wheelchair bound more than one year after the acute phase of AQM. Thus, signs of rhabdomyolysis during the early phase of AQM may indicate a poor prognostic sign of motor function recovery.

In accordance with previous reports at the muscle biopsy level, a decreased myosin:actin protein ratio was observed in the acute phase of AQM and the ratio returned to normal values after 1–2 months recovery, which parallels results of normal ATPase staining and fiber shape after 2 months recovery [7,11,46]. At the single fiber level, on the other hand, myosin content did not return to normal until 8–12 months recovery and actin content returned to normal faster than the myosin content resulting in low myosin:actin ratios during early recovery. The discrepancy between myosin:actin ratios at single fiber and whole biopsy levels may reflect a bias in the selection of single fibers during the dissection procedure. However, these results also show that a significant number of muscle fibers have a pathologically low expression of the motor protein despite normal biopsy myosin:actin ratios. This discrepancy can also help to explain the functional difficulties patients have reported long after their muscle biopsies return to normal [17]. The different single fiber and whole biopsy results also suggest that a significant number of muscle fibers are over-expressing myosin during the early phase of recovery and thereby disguising the low myosin content in other single muscle fibers.

4.2. Myofibrillar protein gene expression

Myosin heavy chain isoforms, i.e., type I and IIa, and actin decreased significantly at the mRNA level during the acute phase of AQM, indicating that protein synthesis is appreciably affected. At 1–2 months recovery, MyHC mRNA levels had increased significantly and a dramatic increase was found after 4–5 months with a 2.5-fold increase above the control value for the IIa MyHC. It is hypothesized that this represents an mRNA overcompensation reflecting an accelerated process of replacing the lost protein. A similar over-compensation of actin mRNA has been reported in rats during recovery from cast immobilization in hindlimb muscles [47]. A significant increase in fetal MyHC was observed at 1–2 months, indicating satellite cell activation and regeneration of the muscle fibers concomitant with increased myofibrillar protein levels.

The down-regulation of myofibrillar protein synthesis at the transcriptional level was not restricted to myosin and a similar change was also observed for the thin filament protein actin. The similar changes in myosin and actin regulation at the transcriptional level, but the significant differences at the protein level, i.e., the preferential loss of myosin, may suggest differences in post-transcriptional regulation or in protein degradation. However, while both myosin and actin have long turnover rates, the turnover rate of actin has been reported to be 2-fold longer than for myosin [48]. The differences in protein expression despite similar changes at the gene level may accordingly be explained by differences in protein turnover rate, although differences in, e.g., translational or protein degradation, cannot be ruled out completely. Nevertheless, the decrease in the synthesis of the proteins, myosin and actin, seems to be a key component of AQM; while it is unclear how this process is initially regulated, although an in-excitable muscle membrane [8,49] and various signal transduction pathways [19,50] have been shown to be affected and/or involved in the development of AQM.

4.3. Myosin binding proteins

The lack of a change in MyBP-C at the mRNA level, but decreased protein expression, indicates that the expression of this myosin associated protein is controlled by a post-transcriptional mechanism. MyBP-C is closely connected to the myosin molecule in the thick filament and the absence or decreased amount of myosin may accordingly result in an enhanced degradation of MyBP-C, although the mechanisms by which each protein decreases may be different. MyHC expression [51] and degradation [24] have been reported to be directly linked to calcium conductance, whereas the overall protein breakdown mechanism implicated in disuse has been the calcium-independent ubiquitin–proteasome pathway [21,23]. Thus, while MyHC synthesis is decreased by low levels of calcium and may be degraded via both the calcium-dependent calpain system and the ubiquitin–proteasome pathway, our results of intact mRNA expression but decreased protein expression for MyBP-C indicate that the MyBP-C protein is most likely degraded via only the ubiquitin–proteasome pathway and unaffected at the synthesis level.

The role of MyBP-H in the muscle during both atrophy and regeneration isunclear. We have previously found an increased MyBP-H expression after 7–13 days of mechanical ventilation and post-synaptic block of neuromuscular transmission in rats [42]. A similar trend was observed in AQM patients during recovery in the present study, both at the mRNA and protein levels. Further, MyBP-H does not completely recede during the acute phase, but appears to be equivalent to the control levels of protein. Both MyBP-H and MyBP-C have been suggested to be involved in the organization and formation of the thick filament [52,53]. In patients with a cardiomyopathy caused by a MyBP-C mutation, MyBP-H has been hypothesized to substitute for the MyBP-C insufficiency [54], it is possible that this is also the case in AQM patients. Another proposed function of MyBP-H is an active role in myosin organization during myofibrillogenesis [55]. MyBP-H may accordingly play a key role in the maintenance of the thick filament structure and/or the reassembly of the thick filament in patients with AQM during the recovery process.

4.4. Recovery

The prolonged weakness associated with the recovery from AQM creates not only a decline in the quality of life [56], but also an increased risk of death, as decreased muscle strength has been found to correlate with increased mortality [57]. Further, it has been found that aged muscles, in comparison with young tissue, do not have the capacity to return to healthy values after a prolonged period of disuse [58], which indicates that many AQM patients will not have the possibility to return to the same quality of life as prior to the disease. The capacity of aged muscle to regenerate, in comparison to young, is greatly decreased as it has been shown that signal transduction factors such as myogenin, MyoD, and IGF-1 are elevated for prolonged periods, and the turnover of the muscle proteins (synthesis and degradation) occurs at a slower rate [59]. If full recovery is possible, it has been shown that periods significantly longer than the time of disuse are required for full recovery to occur [51,60,61], as seen in the presented patients, a recovery time of at least 6–8 months was necessary to begin to return to control levels.

4.5. Sparing of intrafusal fibers

The mechanisms underlying the sparing of both intrafusal muscle fibers and craniofacial muscles in patients with AQM remain unknown. Both cranial nerve innervated muscles and γ-motoneurone innervated intrafusal fibers distinguish themselves with a unique expression of myosin isoforms and combinations of MyHC and MyBP-C isoforms that are not observed in spinal nerve innervated extrafusal muscle fibers [62–67]. Recent gene profiling studies have shown that masticatory muscles, which are non-spinal nerve innervated, display a reduction of the transcripts associated with contractile and cytoskeletal load-sensing

processes [68]. These factors taken together may help to illuminate the differences in response, since the severe muscle wasting, specific to spinal innervated muscles, in patients with AQM is due in part to the unloading caused by the absence of both membrane depolarization and mechanical loading. In AQM, muscles are not depolarized due to the post-synaptic blockade of neuromuscular transmission, an in-excitable muscle membrane, or sedation or a combination of these factors. Further, the lack of both depolarization and weight bearing result in unloading of cytoskeletal and contractile proteins, which results in the activation of specific intracellular signaling pathways, severe muscle wasting and a preferential loss of myosin and myosin-associated proteins in patients with AQM, as well as in an experimental rodent AQM model, separating this muscle atrophy from other muscle wasting conditions [19,42,69,70]. Thus, a difference in the sensitivity to contractile and mechanical loading is forwarded as one possible mechanism underlying the relative sparing of intrafusal muscle fibers and craniofacial muscles.

5. Summary

AQM is a debilitating disease that increases the risk of mortality and severely decreases an individuals' quality of life. The muscle atrophy responsible for the severe weakness is not only a product of increased protein degradation, but also of decreased protein synthesis of myosin and actin at the transcriptional level. To develop successful prevention and intervention strategies, the signaling pathways controlling the decreased mRNA expression, as well as its role in the recovery process, need to be investigated further.

Acknowledgments

We are grateful to Lorraine van Summeren, Helena Svahn, Anna-Stina Höglund, Yvette Hedström and Ann-Marie Gustafsson for excellent laboratory assistance. We are grateful to Dr. Donald Fischman for his generous gift of the myosin binding protein H antibody and to Per Stål for his generous gift of the myosin binding protein C antibody. This study was supported by grants from NIH (AR45627, AR47318, AG014731), AFM, Swedish Cancer Society, and Swedish Research Council (8651) to LL.

References

1. MacFarlane IA, Rosenthal FD. Severe myopathy after status asthmaticus. Lancet 1977 Sep 17;2(8038):615. [PubMed: 71437]
2. Op de Coul AA, Lambregts PC, Koeman J, van Puyenbroek MJ, Ter Laak HJ, Gabreels-Festen AA. Neuromuscular complications in patients given Pavulon (pancuronium bromide) during artificial ventilation. Clin Neurol Neurosurg 1985;87(1):17–22. [PubMed: 3987137]
3. GoochJLSuchytaMRBalbierzJMPetajanJHClemmerTPProlonged paralysis after treatment with neuromuscular junction blocking agents. Crit Care Med1991Sep;19911251131 [PubMed: 1679384]
4. Danon MJ, Carpenter S. Myopathy with thick filament (myosin) loss following prolonged paralysis with vecuronium during steroid treatment. Muscle Nerve 1991 Nov;14(11):1131–1139. [PubMed: 1684024]
5. Hirano M, Ott BR, Raps EC, Minetti C, Lennihan L, Libbey NP, et al. Acute quadriplegic myopathy: a complication of treatment with steroids, nondepolarizing blocking agents, or both. Neurology 1992 Nov;42(11):2082–2087. [PubMed: 1436516]
6. Lacomis D, Smith TW, Chad DA. Acute myopathy and neuropathy in status asthmaticus: case report and literature review. Muscle Nerve 1993 Jan;16(1):84–90. [PubMed: 8423836]
7. Larsson L, Li X, Edstrom L, Eriksson LI, Zackrisson H, Argentini C, et al. Acute quadriplegia and loss of muscle myosin in patients treated with nondepolarizing neuromuscular blocking agents and corticosteroids: mechanisms at the cellular and molecular levels. Crit Care Med 2000 Jan;28(1):34–45. [PubMed: 10667496]
8. Rich MM, Teener JW, Raps EC, Schotland DL, Bird SJ. Muscle is electrically inexcitable in acute quadriplegic myopathy. Neurology 1996 Mar;46(3):731–736. [PubMed: 8618674]

9. al-Lozi MT, Pestronk A, Yee WC, Flaris N, Cooper J. Rapidly evolving myopathy with myosin-deficient muscle fibers. Ann Neurol 1994 Mar;35(3):273–279. [PubMed: 8122880]
10. Sher JH, Shafiq SA, Schutta HS. Acute myopathy with selective lysis of myosin filaments. Neurology 1979 Jan;29(1):100–106. [PubMed: 154627]
11. Matsumoto N, Nakamura T, Yasui Y, Torii J. Analysis of muscle proteins in acute quadriplegic myopathy. Muscle Nerve 2000 Aug;23(8):1270–1276. [PubMed: 10918267]
12. Kupfer Y, Namba T, Kaldawi E, Tessler S. Prolonged weakness after long-term infusion of vecuronium bromide. Ann Intern Med 1992 Sep 15;117(6):484–486. [PubMed: 1354426]
13. Rudis MI, Guslits BJ, Peterson EL, Hathaway SJ, Angus E, Beis S, et al. Economic impact of prolonged motor weakness complicating neuromuscular blockade in the intensive care unit. Crit Care Med 1996 Oct;24(10):1749–1756. [PubMed: 8874316]
14. Mozdziak PE, Pulvermacher PM, Schultz E. Unloading of juvenile muscle results in a reduced muscle size 9 weeks after reloading. J Appl Physiol 2000 Jan;88(1):158–164. [PubMed: 10642376]
15. Mozdziak PE, Pulvermacher PM, Schultz E. Muscle regeneration during hindlimb unloading results in a reduction in muscle size after reloading. J Appl Physiol 2001 Jul;91(1):183–190. [PubMed: 11408429]
16. Kasper CE, Talbot LA, Gaines JM. Skeletal muscle damage and recovery. AACN Clin Issues 2002 May;13(2):237–247. [PubMed: 12011596]
17. Herridge MS, Cheung AM, Tansey CM, Matte-Martyn A, Diaz-Granados N, Al-Saidi F, et al. One-year outcomes in survivors of the acute respiratory distress syndrome. N Engl J Med 2003 Feb 20;348(8):683–693. [PubMed: 12594312]
18. Cheung AM, Tansey CM, Tomlinson G, Diaz-Granados N, Matte A, Barr A, et al. Two-year outcomes, health care use, and costs of survivors of acute respiratory distress syndrome. Am J Respir Crit Care Med 2006;174(5):538–544. [PubMed: 16763220]
19. Di Giovanni S, Molon A, Broccolini A, Melcon G, Mirabella M, Hoffman EP, et al. Constitutive activation of MAPK cascade in acute quadriplegic myopathy. Ann Neurol 2004 Feb;55(2):195–206. [PubMed: 14755723]
20. Lacomis D. Critical illness myopathy. Curr Rheumatol Rep 2002 Oct;4(5):403–408. [PubMed: 12217245]
21. Mitch WE, Goldberg AL. Mechanisms of muscle wasting. The role of the ubiquitin-proteasome pathway. N Engl J Med 1996 Dec 19;335(25):1897–1905. [PubMed: 8948566]
22. Helliwell TR, Wilkinson A, Griffiths RD, McClelland P, Palmer TE, Bone JM. Muscle fibre atrophy in critically ill patients is associated with the loss of myosin filaments and the presence of lysosomal enzymes and ubiquitin. Neuropathol Appl Neurobiol 1998 Dec;24(6):507–517. [PubMed: 9888161]
23. Bodine SC, Latres E, Baumhueter S, Lai VK, Nunez L, Clarke BA, et al. Identification of ubiquitin ligases required for skeletal muscle atrophy. Science 2001 Nov 23;294(5547):1704–1708. [PubMed: 11679633]
24. Showalter CJ, Engel AG. Acute quadriplegic myopathy: analysis of myosin isoforms and evidence for calpain-mediated proteolysis. Muscle Nerve 1997 Mar;20(3):316–322. [PubMed: 9052810]
25. Di Giovanni S, Mirabella M, D'Amico A, Tonali P, Servidei S. Apoptotic features accompany acute quadriplegic myopathy. Neurology 2000 Sep 26;55(6):854–858. [PubMed: 10994008]
26. De Letter MA, van Doorn PA, Savelkoul HF, Laman JD, Schmitz PI, Op de Coul AA, et al. Critical illness polyneuropathy and myopathy (CIPNM): evidence for local immune activation by cytokine-expression in the muscle tissue. J Neuroimmunol 2000 Jul 1;106(1–2):206–213. [PubMed: 10814799]
27. Norman H, Andersson P, Nordquist J, Zackrisson H, Larsson L. Longitudinal measurements of myofibrillar protein and mRNA expression in patients with acute quadriplegic myopathy. The Second New Directions in Skeletal Muscle Biology Meeting. 2006
28. Larsson L, Li X, Edstrom L, Eriksson LI, Zackrisson H, Argentini C, et al. Acute quadriplegia and loss of muscle myosin in patients treated with nondepolarizing neuromuscular blocking agents and corticosteroids: mechanisms at the cellular and molecular levels [see comments]. Crit Care Med 2000;28(1):34–45. [PubMed: 10667496]

29. Frontera WR, Larsson L. Contractile studies of single human skeletal muscle fibers: a comparison of different muscles, permeabilization procedures, and storage techniques. Muscle Nerve 1997 Aug;20(8):948–952. [PubMed: 9236784]
30. Padykula HA, Herman E. The specificity of the histochemical method for adenosine triphosphatase. J Histochem Cytochem 1955 May;3(3):170–195. [PubMed: 14381606]
31. Brooke MH, Kaiser KK. Some comments on the histochemical characterization of muscle adenosine triphosphatase. J Histochem Cytochem 1969 Jun;17(6):431–432. [PubMed: 4241223]
32. Dubowitz, V. Muscle Biopsy: A Practical Approach. London: Tindal & Cox; 1985.
33. Schiaffino S, Gorza L, Pitton G, Saggin L, Ausoni S, Sartore S, et al. Embryonic and neonatal myosin heavy chain in denervated and paralyzed rat skeletal muscle. Dev Biol 1988 May;127(1): 1–11. [PubMed: 3282936]
34. Hughes SM, Cho M, Karsch-Mizrachi I, Travis M, Silberstein L, Leinwand LA, et al. Three slow myosin heavy chains sequentially expressed in developing mammalian skeletal muscle. Dev Biol 1993 Jul;158(1):183–199. [PubMed: 7687223]
35. Larsson L, Moss RL. Maximum velocity of shortening in relation to myosin isoform composition in single fibres from human skeletal muscles. J Physiol 1993 Dec;472:595–614. [PubMed: 8145163]
36. Syrovy I, Hodny Z. Staining and quantification of proteins separated by polyacrylamide gel electrophoresis. J Chromatogr 1991 Sep 13;569(1–2):175–196. [PubMed: 1719011]
37. Giulian GG, Moss RL, Greaser M. Improved methodology for analysis and quantitation of proteins on one-dimensional silver-stained slab gels. Anal Biochem 1983 Mar;129(2):277–287. [PubMed: 6189421]
38. Haddad F, Herrick RE, Adams GR, Baldwin KM. Myosin heavy chain expression in rodent skeletal muscle: effects of exposure to zero gravity. J Appl Physiol 1993 Dec;75(6):2471–2477. [PubMed: 7510278]
39. Tajsharghi H, Thornell LE, Darin N, Martinsson T, Kyllerman M, Wahlstrom J, et al. Myosin heavy chain IIa gene mutation E706K is pathogenic and its expression increases with age. Neurology 2002 Mar 12;58(5):780–786. [PubMed: 11889243]
40. Loughna PT, Morgan MJ. Passive stretch modulates denervation induced alterations in skeletal muscle myosin heavy chain mRNA levels. Pflugers Arch Dec 999;439(1–2):52–55. [PubMed: 10651000]
41. Lu BD, Allen DL, Leinwand LA, Lyons GE. Spatial and temporal changes in myosin heavy chain gene expression in skeletal muscle development. Dev Biol 1999 Dec 1;216(1):312–326. [PubMed: 10588881]
42. Norman H, Nordquist J, Andersson P, Ansved T, Tang X, Dworkin B, et al. Impact of post-synaptic block of neuromuscular transmission, muscle unloading and mechanical ventilation on skeletal muscle protein and mRNA expression. Pflugers Arch 2006;453(1):53–66. [PubMed: 16868767]
43. Hudson LD, Lee CM. Neuromuscular sequelae of critical illness. N Engl J Med 2003 Feb 20;348(8):745–747. [PubMed: 12594320]
44. Friedrich O, Fink RH, Hund E. Understanding critical illness myopathy: approaching the pathomechanism. J Nutr Jul 2005;135(7):1813S, 1817S.
45. Hund E. Neurological complications of sepsis: critical illness polyneuropathy and myopathy. J Neurol Nov 2001;248(11):929–934.
46. Stibler H, Edstrom L, Ahlbeck K, Remahl S, Ansved T. Electrophoretic determination of the myosin/actin ratio in the diagnosis of critical illness myopathy. Intensive Care Med Sep 2003;29(9):1515–1527.
47. Morrison PR, Muller GW, Booth FW. Actin synthesis rate and mRNA level increase during early recoveryof atrophied muscle. AmJ Physiol 1987 Aug;253(2 Pt 1):C205–C209. [PubMed: 3618760]
48. Martin AF. Turnover of cardiac troponin subunits. Kinetic evidence for a precursor pool of troponin-I. J Biol Chem 1981 Jan 25;256(2):964–968. [PubMed: 7451483]
49. Rich MM, Pinter MJ, Kraner SD, Barchi RL. Loss of electrical excitability in an animal model of acute quadriplegic myopathy. Ann Neurol 1998 Feb;43(2):171–179. [PubMed: 9485058]

50. Bodine SC, Stitt TN, Gonzalez M, Kline WO, Stover GL, Bauerlein R, et al. Akt/mTOR pathway is a crucial regulator of skeletal muscle hypertrophy and can prevent muscle atrophy in vivo. Nat Cell Biol 2001 Nov;3(11):1014–1019. [PubMed: 11715023]
51. Desaphy JF, Pierno S, Liantonio A, De Luca A, Didonna MP, Frigeri A, et al. Recovery of the soleus muscle after short- and long-term disuse induced by hindlimb unloading: effects on the electrical properties and myosin heavy chain profile. Neurobiol Dis 2005 Mar;18(2):356–365. [PubMed: 15686964]
52. Welikson RE, Fischman DA. The C-terminal IgI domains of myosin-binding proteins C and H (MyBP-C and MyBP-H) are both necessary and sufficient for the intracellular crosslinking of sarcomeric myosin in transfected non-muscle cells. J Cell Sci 2002 Sep 1;115(Pt 17):3517–3526. [PubMed: 12154082]
53. Yamamoto K. Characterization of H-protein, a component of skeletal muscle myofibrils. J Biol Chem 1984 Jun 10;259(11):7163–7168. [PubMed: 6233279]
54. Gilbert R, Cohen JA, Pardo S, Basu A, Fischman DA. Identification of the A-band localization domain of myosin binding proteins C and H (MyBP-C, MyBP-H) in skeletal muscle. J Cell Sci 1999 Jan;112(Pt 1):69–79. [PubMed: 9841905]
55. Seiler SH, Fischman DA, Leinwand LA. Modulation of myosin filament organization by C-protein family members. Mol Biol Cell 1996 Jan;7(1):113–127. [PubMed: 8741844]
56. Herridge MS. Long-term outcomes after critical illness. Curr Opin Crit Care 2002 Aug;8(4):331–336. [PubMed: 12386494]
57. Metter EJ, Talbot LA, Schrager M, Conwit R. Skeletal muscle strength as a predictor of all-cause mortality in healthy men. J Gerontol A Biol Sci Med Sci 2002 Oct;57(10):B359–B365. [PubMed: 12242311]
58. Zarzhevsky N, Menashe O, Carmeli E, Stein H, Reznick AZ. Capacity for recovery and possible mechanisms in immobilization atrophy of young and old animals. Ann N Y Acad Sci 2001 Apr; 928:212–225. [PubMed: 11795512]
59. Zarzhevsky N, Carmeli E, Fuchs D, Coleman R, Stein H, Reznick AZ. Recovery of muscles of old rats after hindlimb immobilisation by external fixation is impaired compared with those of young rats. Exp Gerontol 2001 Jan;36(1):125–140. [PubMed: 11162917]
60. Hortobagyi T, Dempsey L, Fraser D, Zheng D, Hamilton G, Lambert J, et al. Changes in muscle strength, muscle fibre size and myofibrillar gene expression after immobilization and retraining in humans. J Physiol 2000 Apr 1;524(Pt 1):293–304. [PubMed: 10747199]
61. Maeda H, Kimmel DB, Raab DM, Lane NE. Musculoskeletal recovery following hindlimb immobilization in adult female rats. Bone 1993 Mar–Apr;14(2):153–159. [PubMed: 8334033]
62. Bredman JJ, Wessels A, Weijs WA, Korfage JA, Soffers CA, Moorman AF. Demonstration of‘cardiac-specific’ myosin heavy chain in masticatory muscles of human and rabbit. Histochem J 1991 Apr;23(4):160–170. [PubMed: 1836206]
63. Fischer MD, Budak MT, Bakay M, Gorospe JR, Kjellgren D, Pedrosa-Domellof F, et al. Definition of the unique human extraocular muscle allotype by expression profiling. Physiological genomics 2005 Aug 11;22(3):283–291. [PubMed: 15855387]
64. Korfage JA, Koolstra JH, Langenbach GE, van Eijden TM. Fiber-type composition of the human jaw muscles — (part 1) origin and functional significance of fiber-type diversity. J Dental Res 2005 Sep;84(9):774–783.
65. Korfage JA, Van Eijden TM. Myosin isoform composition of the human medial and lateral pterygoid muscles. J Dental Res Aug 2000;79(8):1618–1625.
66. Liu JX, Eriksson PO, Thornell LE, Pedrosa-Domellof F. Myosin heavy chain composition of muscle spindles in human biceps brachii. J Histochem Cytochem 2002 Feb;50(2):171–183. [PubMed: 11799136]
67. Yu F, Stal P, Thornell LE, Larsson L. Human single masseter muscle fibers contain unique combinations of myosin and myosin binding protein C isoforms. J Muscle Res Cell Motil 2002;23(4):317–326. [PubMed: 12630706]
68. Evans M, Morine K, Kulkarni C, Barton ER. Expression profiling reveals heightened apoptosis and supports fiber size economy in the murine muscles of mastication. Physiological Genomics 2008 Sep 17;35(1):86–95. [PubMed: 18593863]

69. Larsson L, Li X, Berg HE, Frontera WR. Effects of removal of weight-bearing function on contractility and myosin isoform composition in single human skeletal muscle cells. Pflugers Arch Jun 1996;432(2):320–328. [PubMed: 8662283]

70. Nordquist J, Hoglund AS, Norman H, Tang X, Dworkin B, Larsson L. Transcription factors in muscle atrophy caused by blocked neuromuscular transmission and muscle unloading in rats. Mol Med (Cambridge, Mass 2007 Sep–Oct;13(9–10):461–470. [PubMed: 17622304]

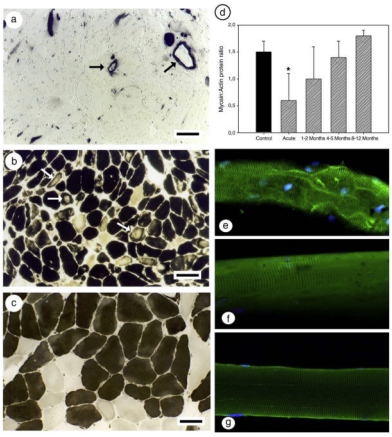

Fig. 1.

mATPase staining and myofibrillar protein expression during the acute phase of AQM and during recovery. (a–c) mATPase staining after acid preincubation (pH 4.6) in three different patients with AQM in the acute phase [7]. Arrows indicate the strong straining in the blood vessel walls (a) and regional loss of mATPase staining (b). A cross-section from a patient with a myosin:actin ratio corresponding to 0.6 with only minimal changes in the mATPase staining (c); the horizontal bars represent 100 μm. (d) Myosin:actin ratio as determined by 12% SDS-PAGE (Control = filled bar; AQM patients = hashed bar. Statistical significance versus controls is denoted by * ($p<0.05$); (e–g) single muscle fibers stained for myosin and myonuclei from the acute phase (e), 8 months recovery (f), and a control fiber (g; 40×).

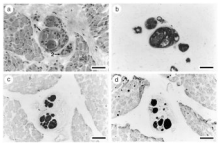

Fig. 2.

Intrafusal muscle fibers in muscle spindles from a patient in the acute phase with general myosin loss in extrafusal muscle fibers and maintained myosin expression in intrafusal muscle fibers. Note the severe muscle fiber atrophy of extrafusal compared with intrafusal muscle fibers. Serial sections stained for hematoxylin-eosin (a; arrows indicate muscle spindles), mATPase after acid preincubation (b; pH 4.6), and immunocytochemical stainings with mAbs reactive with fast (c) and slow (d) MyHCs.

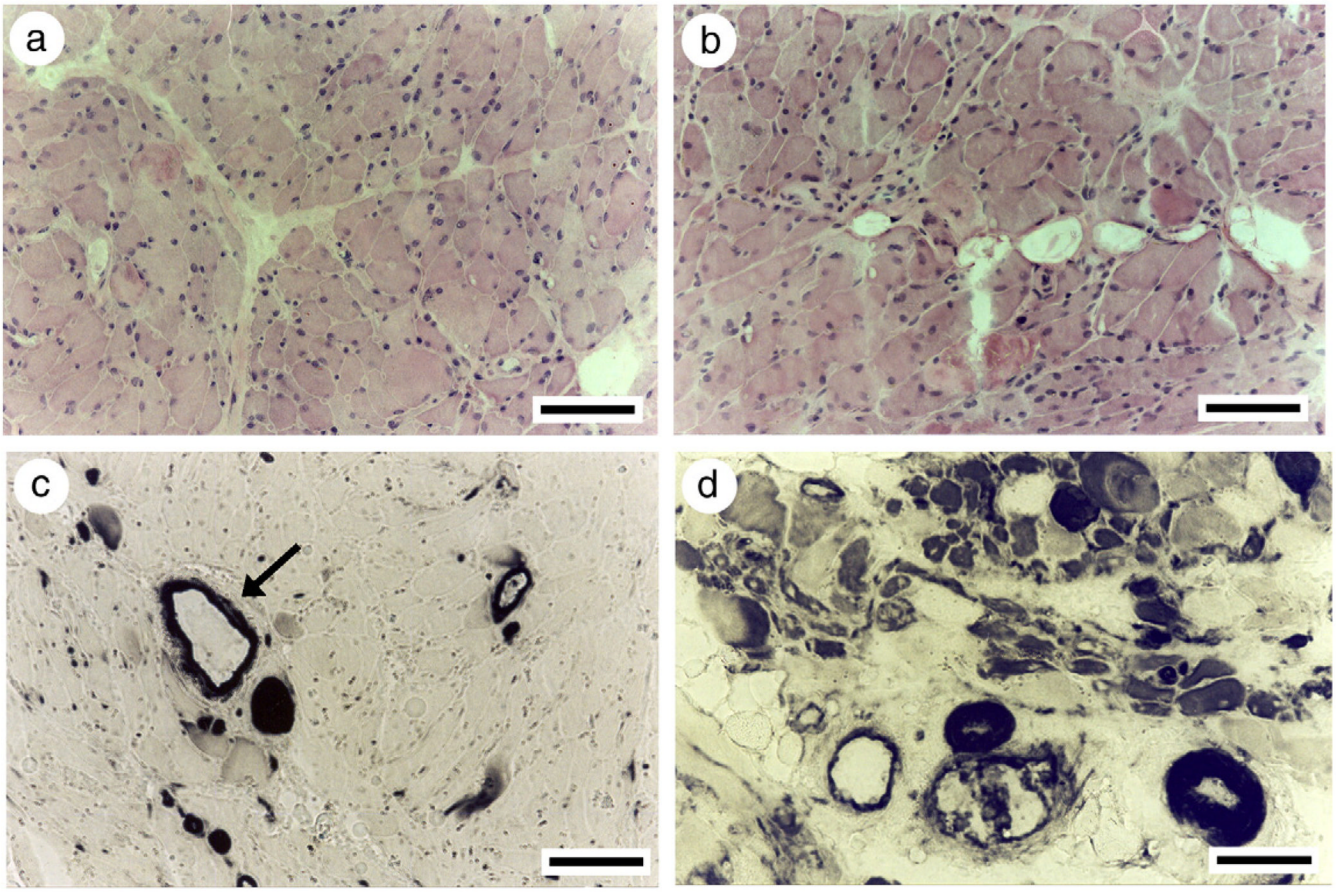

Fig. 3.
Hematoxylin-eosin (a, b) and mATPase stainings after acid preincubation (pH 4.6; c, d) in a patient with AQM (M1) at the acute stage (a, c) and during early recovery (b, d). Arrow denotes the presence of myosin in vascular tissue.

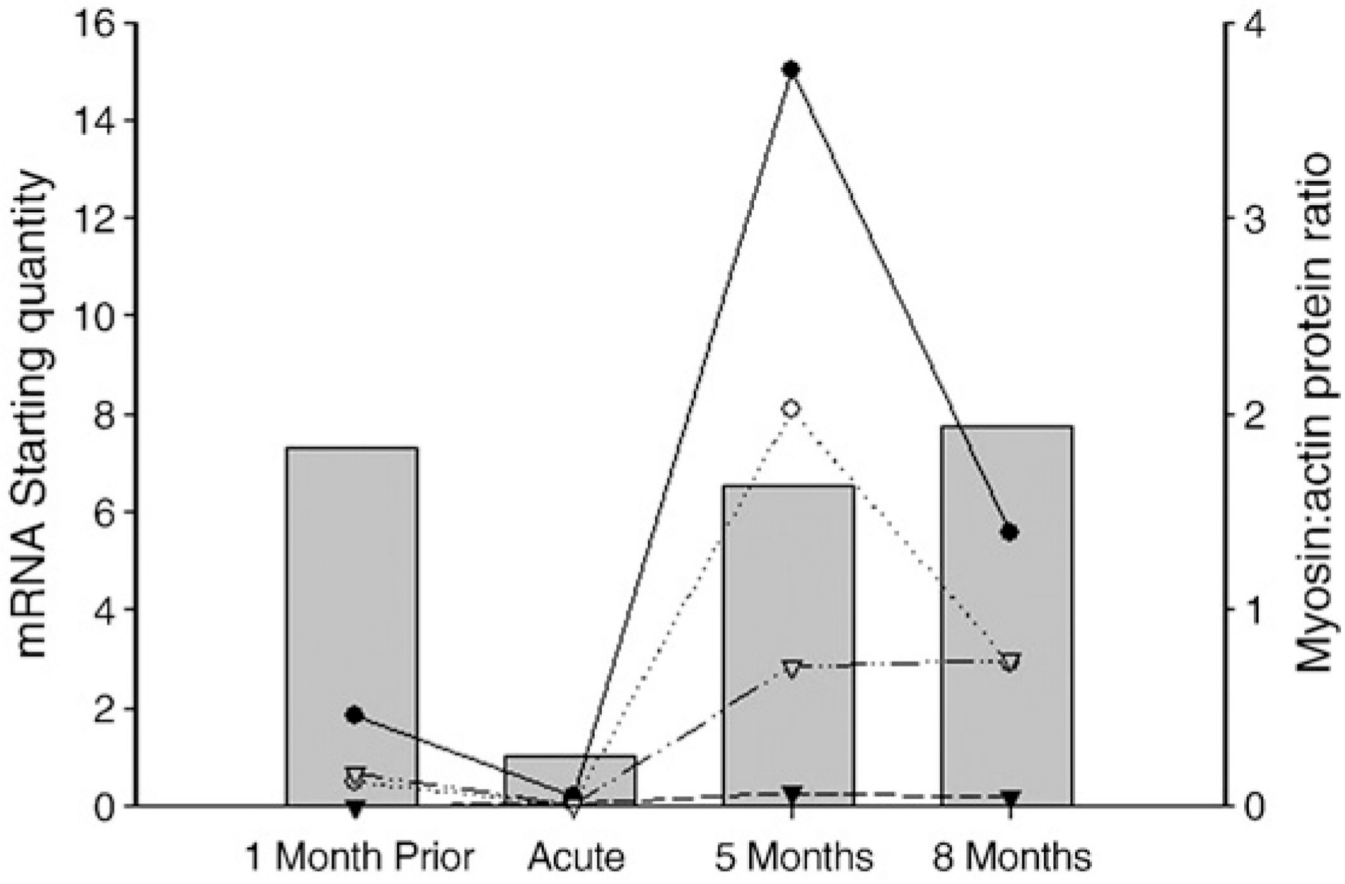

Fig. 4.

Myofibrillar protein, myosin heavy chain, mRNA expression (left *Y*-axis) and myosin:actin protein ratios from a whole biopsy (right *Y*-axis) in a patient with AQM (M7) from whom muscle samples were collected prior to ICU admission, in the acute phase and during the recovery process. Expression of MyHCIIa (filled circles), MyHCI (open circles), fetal MyHC (filled triangles), and actin (open triangles) mRNA are represented by lines (values are mRNA starting quantity). Myosin:actin protein ratio is represented by grey filled bars.

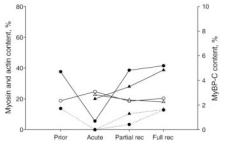

Fig. 5.

MyHC (filled symbols, solid lines), actin (open symbols, solid lines) and MyBP-C (filled symbols, dotted lines) contents normalized to total protein content in muscle biopsies from two patients followed longitudinally from the acute phase with muscle paralysis, during partial recovery to full, or near full, recovery. In one of these patients, a muscle biopsy was taken approximately 1 month prior to the acute phase (circles) and in the other patient at three different time points (triangles).

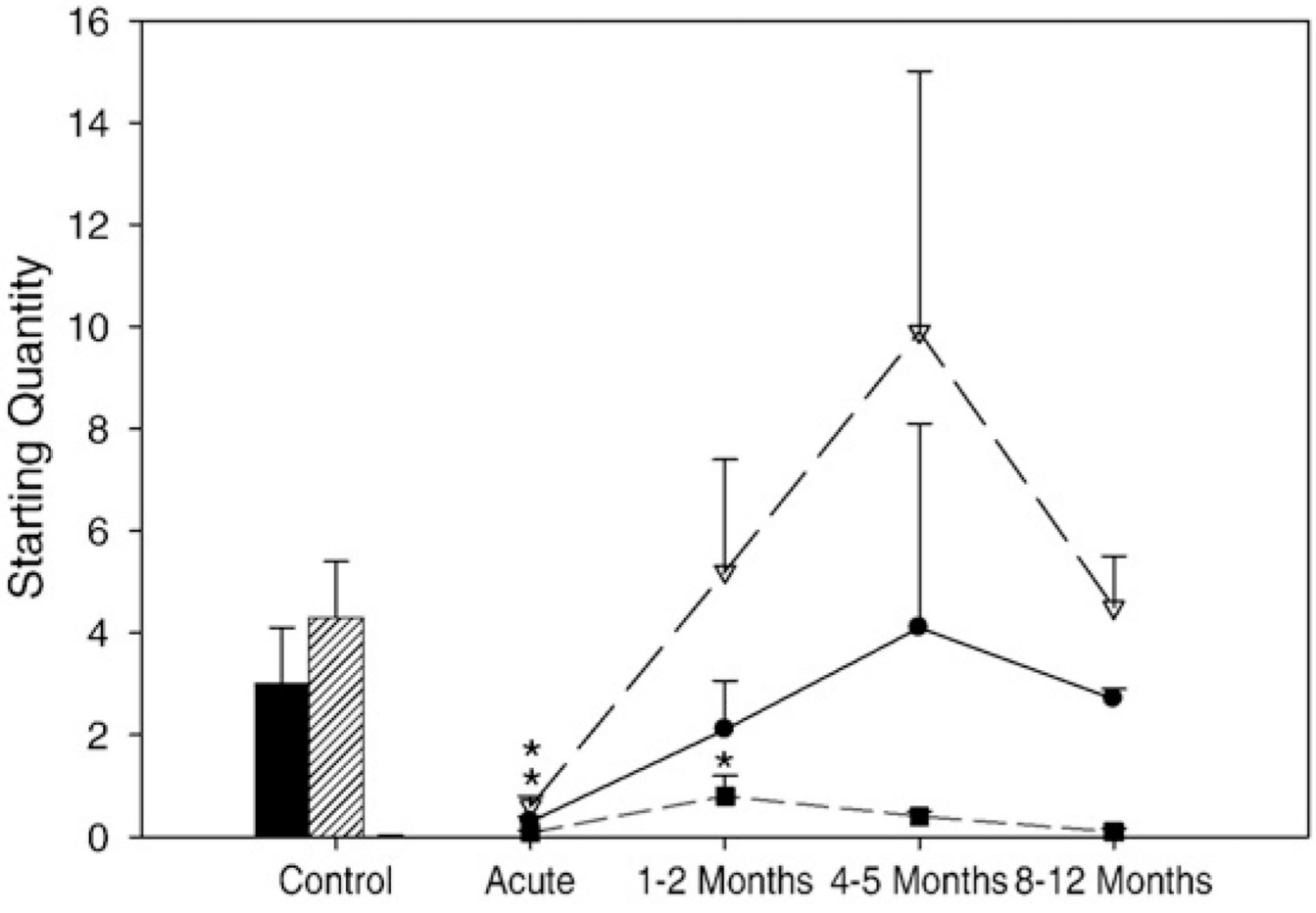

Fig. 6.

mRNA expression for the type I (control: black bar; patients: line with filled circles), IIa (Control: hashed bar; Patients: line with open triangles), and fetal (gray bar and line with filled squares) MyHCs. Values are starting quantity±standard error. Statistically significant differences versus controls is denoted by * ($p<0.05$).

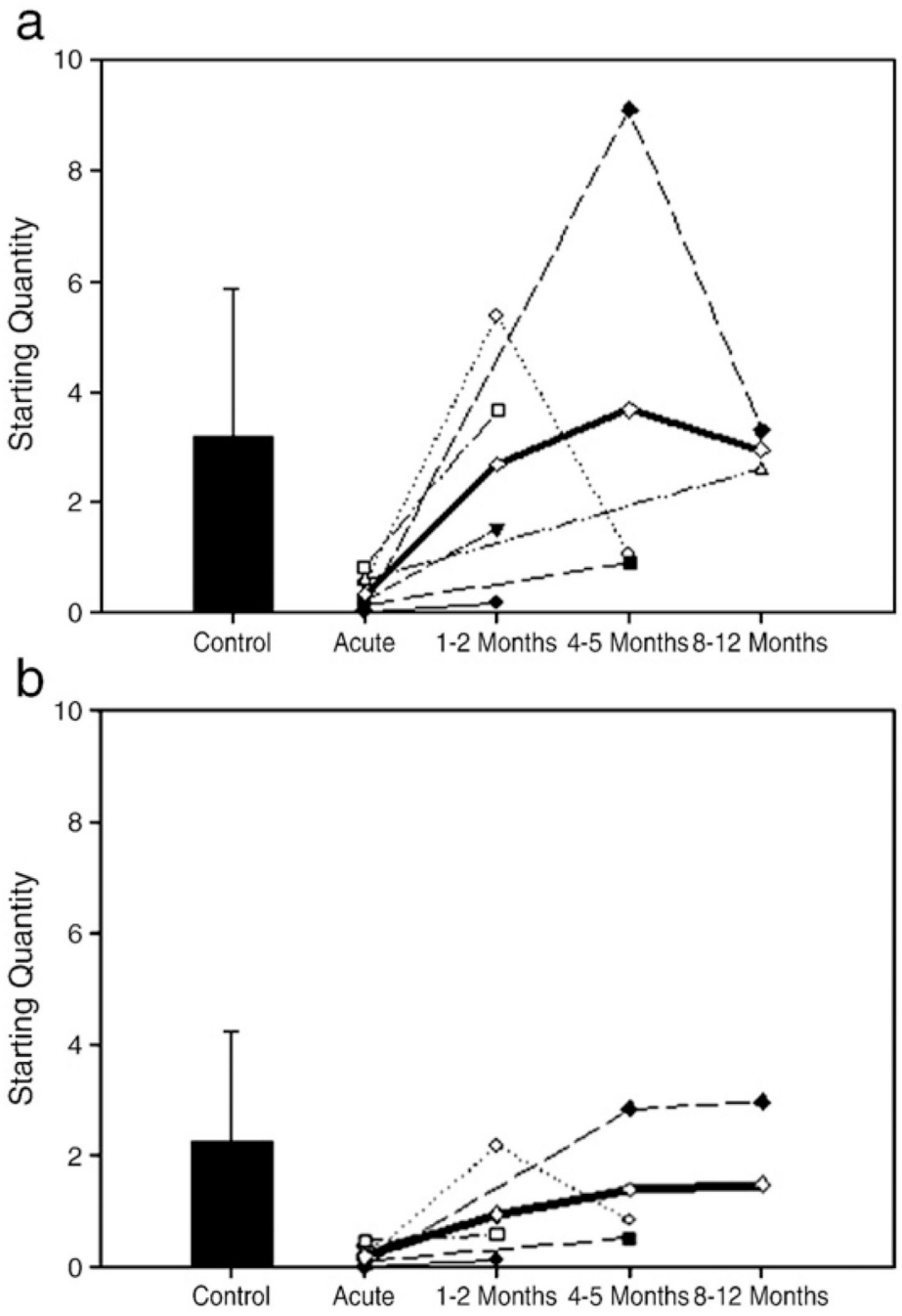

Fig. 7.

Total MyHC mRNA (A) and actin mRNA (B) content in the different AQM patients (M1 – filled circle; M2 – open circle; M3 – filled triangle; M4 – open triangle; M5 – filled square; M6 – open square; M7 – filled diamond; Average of all patients – open diamond) and controls (filled bar±standard deviation).

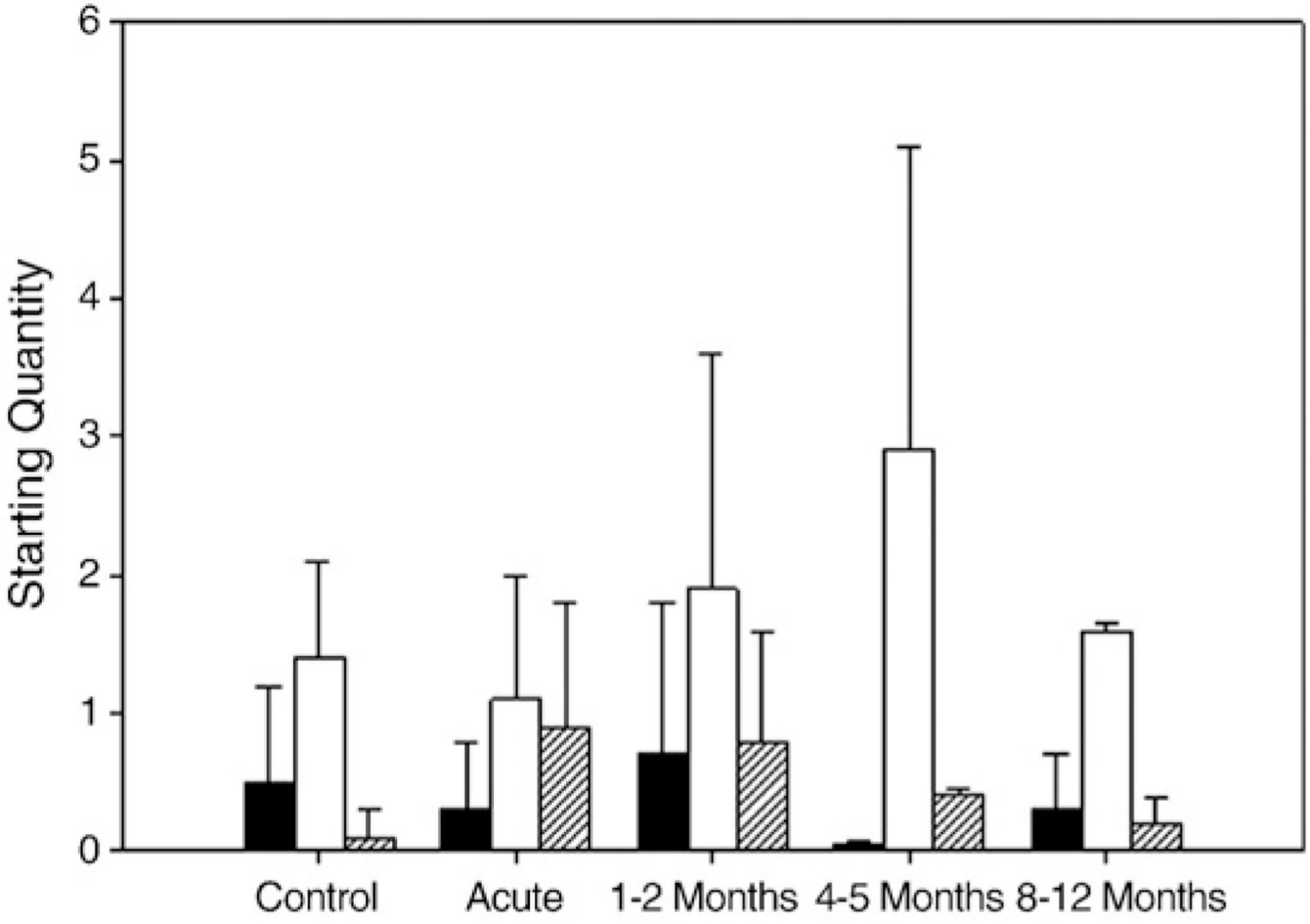

Fig. 8.
Myosin binding protein mRNA expression. MyBP-C_{fast} (open bars), MyBP-C_{slow} (filled bars), and MyBP-H (hashed bars). Values are starting quantity±standard deviation.

Table 1

AQM patient synopsis.

ID	Age	Sex	Days on mechanical ventilation*	History	Pharmacology	Neurological exam	Symptoms	Days of biopsy	Diagnosis	Recovery
M1	70	F	14	Chronic respiratory insufficiency and long-term steroid treatment	CS, NMBA, antibiotics	Absence of deep tendon reflexes, normal SNAP, absent/low CMAP	Muscle weakness, preserved cranial innervated muscle function	20, 39	AQM	Deceased 2 months post-discharge
M2	62	M	28	Bilateral pneumonia, ARDS	CS, NMBA, antibiotics	Absent deep tendon reflexes, normal SNAP, normal conduction velocities, decreased CMAP	Muscle weakness, preserved cranial innervated muscle function	20, 50, 17 8	AQM	Full neural recovery 6 months post discharge
M3	58	F	18	Unilateral pneumonia	CS, NMBA, antibiotics	Absent deep tendon reflexes, normal conduction velocities, low CMAPs	Complete quadriplegia, intact cranially innervated muscle function	25, 64	AQM	Partial recovery and deceased
M4	61	M	–	Diabetes mellitus, hypertonia, asthma and septicemia	CS, NMBA, antibiotics	Absent deep tendon reflexes, absent SNAP, normal sensory nerve conduction velocity	Quadriplegia, intact function of cranial nerve innervated muscles	41, 365	AQM	Full recovery 12 months post-discharge
M5	67	F	12	Obstructive cardiomyopathy, sepsis	CS, NMBA, antibiotics	Absent deep tendon reflexes in the legs, normal nerve conduction velocities	Complete quadriplegia	22, 148	AQM	Partial recovery
M6	75	F	11	Surgery (brain)	CS	Low CMAP, normal SNAP	Complete quadriplegia, intact cranially innervated muscle function	–	AQM	–
M7	67	M	9	Mild muscle soreness and respiratory distress	CS, NMBA	Absent deep tendon reflexes, normal sensory nerve conduction velocities, slightly lower than normal SNAP and motor conduction velocities, absent/low CMAP	Quadriplegia, intact function of cranial nerve innervated muscles	−21, 35, 267	AQM	Full recovery 12 months post-discharge

*Days on mechanical ventilation refers to the days prior to the initial diagnosis of AQM.

Table 2

Single fiber protein analyses.

		M 1	M 2	M 3	M 4	M 5	M6	M 7	Average	Control
Acute	100×(myosin (ng)/ total protein (ng))	0 ± 0***	2.8 ± 4.5***	0 ± 0***	0.1 ± 0.3***,§	3.8 ± 3.3***	0.4 ± 0.5***	0 ± 0***,§	1.5 ± 2.9***,§	16.4 ± 8.9
	100×(actin (ng)/ total protein (ng))	11.4 ± 3.8	6.7 ± 2.1**	0 ± 0***	6 ± 5.1	7 ± 4.4	1 ± 0.3***	5 ± 4.9***,§	5.0 ± 5.0***,§	10.6 ± 3.8
	Ratio (myosin/actin)	0 ± 0***	0.4 ± 0.6***	0 ± 0***	0 ± 0.1***,§	0.4 ± 0.3***	0.4 ± 0.4***	0 ± 0***,§	0.2 ± 0.4***,§	1.6 ± 0.5
	Whole biopsy Gel Ratio (myosin/actin)	0.09	1.1	0.14	1.3	0.6	0.42	0.3	0.6 ± 0.5	1.6
1–2 months	100×(myosin (ng)/ total protein (ng))	0 ± 0***	2.9 ± 3.7 ***	0 ± 0***	–	–	–	–	2.0 ± 3.3***,§	–
	100×(actin (ng)/ total protein (ng))	7.1 ± 4.3*	7.3 ± 4.2**	9.1 ± 14.7	–	–	–	–	7.8 ± 8***,§	–
	Ratio (myosin / actin)	0 ± 0***	0.3 ± 0.4***	0 ± 0***	–	–	–	–	0.2 ± 0.3***,§	–
	Whole biopsy gel ratio (myosin/actin)	0.62	0.7	1.8	–	–	0.74	–	1.0 ± 0.6	–
4–5 months	100×(myosin (ng)/ total protein (ng))	–	4.1 ± 6.0***	–	–	1.1 ± 2.4***	–	1.6 ± 2.5***,§	2.5 ± 4.3***,§	–
	100×(actin (ng)/ total protein (ng))	–	7.5 ± 6.1***	–	–	25.9 ± 42.4	–	4.5 ± 5.2***,§	10.5 ± 19.8***,§	–
	Ratio (myosin/actin)	–	0.4 ± 0.6***	–	–	0.01 ± 0.02***	–	0.3 ± 0.6***,§	0.3 ± 0.5***,§	–
	Whole biopsy gel ratio (myosin/actin)	–	–	–	–	1.2	–	1.6	1.4 ± 0.3	–
8–12 months	100×(myosin (ng)/ total protein (ng))	–	–	–	15.6 ± 8.2	–	–	17.8 ± 5.1	16.7 ± 1.6	–
	100×(actin (ng)/ total protein (ng))	–	–	–	10.2 ± 3.4	–	–	16.9 ± 9.6	13.6 ± 7.8	–
	Ratio (myosin/actin)	–	–	–	1.4 ± 0.6	–	–	1.3 ± 0.6	1.4 ± 0.6	–
	Whole biopsy gel ratio (myosin/actin)	–	–	–	1.7	–	–	1.9	1.8 ± 0.1	–

Myosin and actin protein concentrations, and myosin:actin protein ratios, related to total protein, in single fibers, as well as myosin:actin ratios in whole biopsies for patients M1–M7 during the acute stage and subsequent recovery phases and controls. Myosin and actin values were obtained from 12% SDS-PAGE. Values are mean±SD. Statistically significant differences versus the control group is denoted * (p<0.05), ** (p<0.01), and *** (p<0.001), and versus the 8–12 month recovery time point is denoted § (p<0.001).

Table 3

Primer and probes for real-time PCR.

Gene	Forward primer	Probe	Reverse primer	Expected
MyHCIIa	AAACCCTGAAGCGAGAGAACAA	CAGAGGAGATTTCTGACCTCACGGAAC	TCATGGATACGTTTCCCTCCTT	88
MyHCIIx	CAAAGGTGAAATCCTACAAGAGACAA	AAGAAGCGGAGGAACAATCCAACGTCA	TGGATCCTCCGGAATTTGG	82
MyHCI	CTCGCTCCCTCAGCACAGA	TGGAACATCTGGAGACCTTCAAGCGG	CTGCTCAGTCAAGTCGGAGATCT	125
Embryonic MyHC	GGACAGGAAGAATGTGCTGAGAATT	ATCTGGTGGATAAACTG	GCCTCTTGTAGGACTTGACTTTCAC	78
Fetal MyHC	TCTGCGTATCCAGCTTGAGTTAAA	CAAGTCAAGTCTGAAGTTG	CTCATCCTTTTCTGCGATTTTTCT	70
α-actin	CTACCCGCCCAGAAACTAGACA	ACCACCGCCCTCGTGTGCG	CCAGGCCGGAGCCATT	79
MyBP-C fast	TGGAGTGGTTCAACGTCTATGAAC	Sybr Green®	CCACGATAAGGTCGGACACAGTA	66
MyBP-C slow	GAAGAACACCAAACCCAGTGAGTA	Sybr Green®	CGCTGCAGGTCGGTGATT	65
MyBP-H	CAAATACCGCGCCCTCTCT	Sybr Green®	CAGGTGTAGACCCCAGAATCAAA	84
28S	GGGAGAGGGTGTAAATCTCGC	CCGGGCCGTACCCATATCCGC or Sybr Green®	CTGTTCACCTTGGAGACCTGC	65